Eur. Phys. J. D (2015) 69: 212
DOI: 10.1140/epjd/e2015-60116-6

THE EUROPEAN PHYSICAL JOURNAL D

Regular Article

Geometrical shapes, stabilities and electronic behavior of small Fe_xSn_y ($x + y \leq 5$) atomic clusters

Elisa Marina Sosa-Hernández[1], Juan Martín Montejano-Carrizales[2,a], and Pedro Gilberto Alvarado Leyva[3]

[1] DICIM, Facultad de Ciencias, Universidad Autónoma de San Luis Potosí, Álvaro Obregón 64, 78000 San Luis Potosí, S.L.P., México
[2] Instituto de Física Manuel Sandoval Vallarta, Universidad Autónoma de San Luis Potosí, Álvaro Obregón 64, 78000 San Luis Potosí, S.L.P., México
[3] Departamento de Física, Facultad de Ciencias, Universidad Autónoma de San Luis Potosí, Álvaro Obregón 64, 78000 San Luis Potosí, S.L.P., México

Received 19 February 2015 / Received in final form 22 July 2015
Published online 15 September 2015 –

Abstract. We report the results of DFT calculations wich were performed to investigate equilibrium structures, electronic properties and stability of small free Fe_xSn_y clusters with $x + y \leq 5$ within the framework of density functional theory as implemented in SIESTA code. We find that optimized structures of these binary clusters prefer geometries with high coordinations and show significant variations as compared to that of the pure clusters; all the clusters show magnetic behavior independently of the Fe concentration, the antiferromagnetic-like coupling betwen Fe-Sn is present generally. Also the electronic behavior is analized through the ionization potential, the electron affinity, the hardness and the HOMO-LUMO gap.

1 Introduction

In recent years, the study of nanoalloys has become an important tool in nanoengineering for several technologically promising fields, for example in catalysis; so far most of the studies have focused mainly on the changes observed in chemical activity or in the magnetic and optical properties with the changes in particle size and in their chemical composition. Alloying in bulk systems is well understood, alloying at the nanoscale has been little explored; questions as what controls the structural, electronic and chemical properties of bimetallic nanoparticles (BNP) remain unanswered. The interaction between the two components of BNP introduces a mutual influence on neighboring atoms which leads to the unique properties of these systems not found in other regime size. Experimentally and theoretically it has been clearly stablished that the properties of BNP are not necessarily given by the average behavior of their corresponding isolated constituents.

The research in the field of BNP is exciting due to their potential applications in the automobile industry and hydrocarbon reactions as catalysts [1,2]. The bimetallic atomic clusters are into BNP, these systems are currently of great interest due they have an important role, not only in the miniaturization of devices but also in the fundamental understanding of materials at nanoscale. BNP with novel properties such as enhanced stability by suitable doping, tunable gaps and optical properties could lead to novel nanoscale optoelectronics as well as miniature spintronics and storage devices. The conceivable geometrical arrangements for a BNP is determined by the different radii of its elements; in addition, the number of possible structures is increased by the relative positions of the constituent atoms within the given stoichiomestry.

In recent years, an important effort has been devoted to the study of bimetallic atomic clusters [3]. By adding a second element to monoatomic clusters, the composition and spatial distribution of the components provide additional parameters that modify their physical and chemical properties and open the possibility of synthesizing a wider set of novel materials. In particular, due to their potential applications, atomic clusters containing magnetic elements are presently subject of intense research, the interest in binary clusters based mainly on transition metals (TM) atoms where the second element can be a metal (TM, Au, Ag), a semiconductor or a rare earth is increasing. From the point of view of the magnetic properties, an interesting result is that by coating TM atoms one can achieve an enhancement in the magnetic moments of TM atoms [4–6]. Another result about BNP is that they can replace the iron oxide particles as magnetic carriers in vitro separation and therapeutic in vivo technology [7].

BNP with Sn as a component have been studied widely, for example, in the study of structural evolution of doped gold clusters [8]; in cage encapsulating TM atoms [9]; in cages in endohedral stannaspherenes forms [10] and in the study of mobility of Sn atoms in

[a] e-mail: jmmc@dec1.ifisica.uaslp.mx

Cu_2Sn surface alloy [11]. In particular, atomic clusters FeSn can be produced by direct reaction of individual atoms in a solid rare-gas matrix at low temperature [12], where the authors characterized the various dimers and trimers of FeSn clusters.

The remainder of the paper is organized as follows: in the next section the computational method used here is briefly recalled. Results for the local magnetic moments and the global minimum structures of Fe_xSn_y with $x+y \leq 5$ clusters are presented and discussed in Section 3; finally Section 4 summarizes the main conclusions.

2 Computational details

The Spanish initiative for electronic simulation of thousands atoms (SIESTA) [13] is a code developed within the density functional theory, that uses a linear combination of pseudo-atomic orbitals as a basis sets. The electronic core is replaced by a non-local conserving Troullier-Martins pseudopotential [14] that is factorized in the Kleinman-Bilander form [15]. By means of this code one can perform in addition to the electronic calculations, structural optimizations in different ways, like conjugate gradients or the Verlet algorithm, which has been successfully applied to a variety of systems, like surfaces, absorbates, biological molecules and free supported clusters.

In this contribution we have used the generalized gradient approximation (GGA) as a parametrized by Perdew-Burke-Ernzerhof [16] for the exchange-correlation potential. The pseudo-potentials are considered using the natural electronic configuration, for Sn atom $5s^2 5p^2$. For Fe atom we have used the atomic configuration $3d^7 4s^1$, previous studies of Fe in different environments suggest this configuration as adequate for building a transferable pseudo-potential [17]. The valence states were described using a double-ζ polarized basis set for Fe whereas for Sn a double-ζ was considered. In calculations, the clusters were placed in a supercell cubic of a side size of 20 Å. This cell is large enough to warranty that: (a) the interactions between the cluster and its replicas in neighboring cells are negligible, (b) it is sufficient to consider only the γ point when integrating over the Brillouin zone.

The energy cutoff used to define the real space grid for the numerical calculations involving the electron density was 250 Ry. Furthermore, by using a conjugate gradient method, all the structures were fully relaxed without geometry or spin constrains until the forces were smaller than 0.003 eV/Å.

It is worth to notice that we have considered linear, planar and three-dimensional geometries and we have tested different spin isomers in all cases to be sure that the ground state was obtained for the electronic properties in our calculations; the previous due to the sensitivity of the magnetic properties to the structure and chemical order [18]. However, the situation for alloy clusters is quite cumbersome as one has to deal a large number of starting geometries because of the presence of homotops, i.e., geometrical structures with the same number of atoms and composition, but differ in the arrangement of the doped atom, so the variety of structures in alloy clusters is larger than that in pure clusters.

Table 1. Our simulation GGA-PBE compared with other DFT theoretical approaches and experimental results for average magnetic moment $\bar{\mu}(\mu_B)$, binding energy per atom E_b (eV/atom), and average interatomic distance d (Å/bond), in pure Fe clusters.

x	$\bar{\mu}$	$\bar{E}_b$	$\bar{d}$	Method
2	3.00	1.41	2.04	This work
	3.00	2.25	1.96	SIESTA-LSDA [22]
	3.00	1.59	2.02	DMOL-BLYP [23]
		1.30	1.87–2.02	Exp. [24,25]
3	3.33	1.89	2.22	This work
	3.33	1.94		DMOL-BLYP [23]
	2.67	2.67	2.14	SIESTA-LSDA [22]
4	3.5	2.28	2.40	This work
	3.5	2.22		DMOL-BLYP [23]
	3.00	3.13	2.33	SIESTA-LSDA [22]
5	3.6	2.58	2.18	This work
	3.6	2.55		DMOL-BLYP [23]
	3.2	3.48	2.47	SIESTA-LSDA [22]

3 Results for pure Fe and Sn clusters

The first step toward the theoretical modeling of atomic clusters is to determine their ground state structures; to obtain the minimum energy structures (MES) we consider several starting geometries and allowed each one of the geometries to relax for all possible collinear spin configurations.

3.1 Pure clusters

In order to test the validity of the pseudo-potentials used here, we calculated the binding energy and the interatomic distance of the different pure clusters, in Tables 1 and 2, we present the results for pure Fe clusters and pure Sn clusters with 2−5 atoms, respectively. Our results are compared with some theoretical and experimental values published in the literature. For Fe_2 dimer, all the calculations give the same average magnetic moment and similar interatomic distances (comparable with the experimental ones). Our average binding energy compares well with the experimental result as well as with the obtained with other DFT methods, but is smaller than the obtained with SIESTA-LSDA (local spin density approximation). For the triangle, there is more dispersion in the results of different DFT approaches. In general, the GGA calculations lead to higher magnetic moments and lower binding energy than the LSDA ones. These tendencies are mantained for Fe_4 and Fe_5 clusters, from Table 1 we can notice a good agreement between our results with the DMOL-BLYP calculations.

Table 2. Our simulation GGA-PBE compared with other DFT theoretical approaches and experimental results for binding energy per atom (eV/atom), $\bar{E}_b$, and average interatomic distance (Å/atom), $\bar{d}$, in pure Sn clusters.

y	$\bar{E}_b$	$\bar{d}$	Method
2	1.13	2.82	This work
	1.18		GGA-RPBE [26]
	1.25	2.75	G03-B3LYP [19]
	1.20	2.78	GGA [27]
	1.01		Exp. [28]
		2.75	Exp. [29]
3	1.70	2.93	This work
	1.66		GGA-RPBE [26]
	1.77	2.84	G03-B3LYP [19]
	1.77	2.68	GGA [27]
	1.72		Exp. [28]
4	2.08	2.94	This work
	2.09		GGA-RPBE [26]
	2.48	2.86	G03-B3LYP [19]
	2.22	2.83	GGA [27]
	1.98		Exp. [30]
5	2.11	2.97	This work
	2.26		GGA-RPBE [26]
	2.34	3.18	G03-B3LYP [19]
	2.40	2.83	GGA [27]
	2.10		Exp. [30]

For Sn_2 we found a dimer with an average magnetic moment of 2 μ_B and a bond length of 2.82 Å, this value is above about 0.06 Å, as compared with other DFT results, and 0.07 Å, as comparing with the experimental result, whereas our result for binding energy per atom is in good accordance with the experimental result as well as with the obtained with the GGA-RPBE result. We can notice the largest value for the binding energy per atom corresponds to B3LYP method [19], the authors used a basis set including relativistic effects. Balasasubramanian et al. [20] studied Sn_2 cluster introducing spin-orbit interaction at the configuration interaction scheme, their result for E_b is 1.02 eV/atom. But as can see below, our method give reasonable results for average binding energy for larger Sn clusters. In Figure 1, the lowest energy structures for pure Fe and Sn clusters are shown. We can notice that equilibrium structures of Sn clusters diverge significantly from those of the corresponding crystalline fragments due to severe broken bonds but share similar structures with Si and Ge nanoclusters, which are consistent with experimental results [21].

From Table 2, our results for $\bar{E}_b$ are in best concordance with the experimental results that other DFT approaches but our bond lengths are overstimated with respect to the same DFT studies for all the Sn clusters studied here.

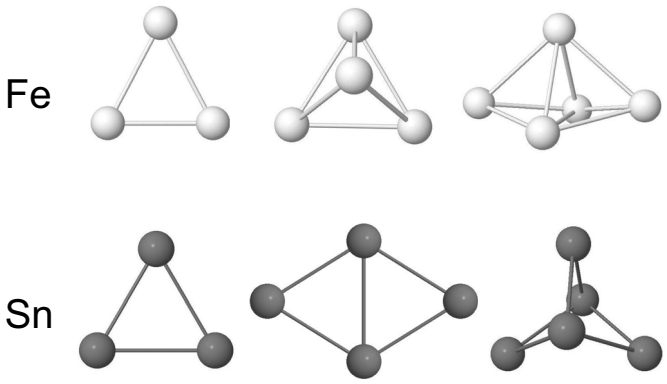

Fig. 1. Illustration of the lowest energy structures for pure clusters with three to five atoms.

In resume, we can conclude that our DFT approach leads to a good overall agreement with the other methods as well as with the experiments (when available) for the pure Fe and Sn clusters, with regard to the binding energies, magnetic moments and interatomic distances. Therefore, this gives us confidence in the accuracy of our method for the study of FeSn nanoalloys of similar sizes.

3.2 Doped clusters

In this section we present the MES, stability and magnetic moments of the free Fe_xSn_y clusters with $x + y \leq 5$. For the FeSn dimer, the ground state presents an antiferromagnetic-like order with a local magnetic moments $\mu(\mathrm{Sn}) = -1.449\,\mu_B$ and $\mu(\mathrm{Fe}) = 3.449\,\mu_B$. Our calculations give a binding energy per atom, E_b of 1.386 eV/atom; this value is higher than the value for pure Sn_2 cluster and is approximately the same value for Fe_2 dimer.

The first excited state is above of the ground state in 0.42 eV in total energy, in this cluster the local magnetic moments point in the same direction, giving a ferromagnetic-like order; our calculations show an enhanced local Fe moment of 3.557 μ_B and the local Sn moment is diminished to 0.443 μ_B.

Our Mulliken population analysis shows a charge transference from Sn atom to Fe atom, this result is concording with the experiment [12], by using Mösbauer effect.

In Figure 2, we present the MES ($\Delta E_T = 0.0$) and the first isomers ($\Delta E_T > 0.0$), in order to found the ground state we considered different geometries with different spin states for all the concentrations considered here. From this Figure we can obtain information about the total energy, local magnetic moments, total magnetization, the value of the binding energy per atom and the average bond length for each cluster studied here.

For clusters with 3 atoms, $FeSn_2$ and Fe_2Sn, we considered only triangular arrangements due to this geometry is common for the homonuclear clusters, see Figure 1. In both clusters, the MES corresponds to an isosceles triangle, these results are in concordance with the structures

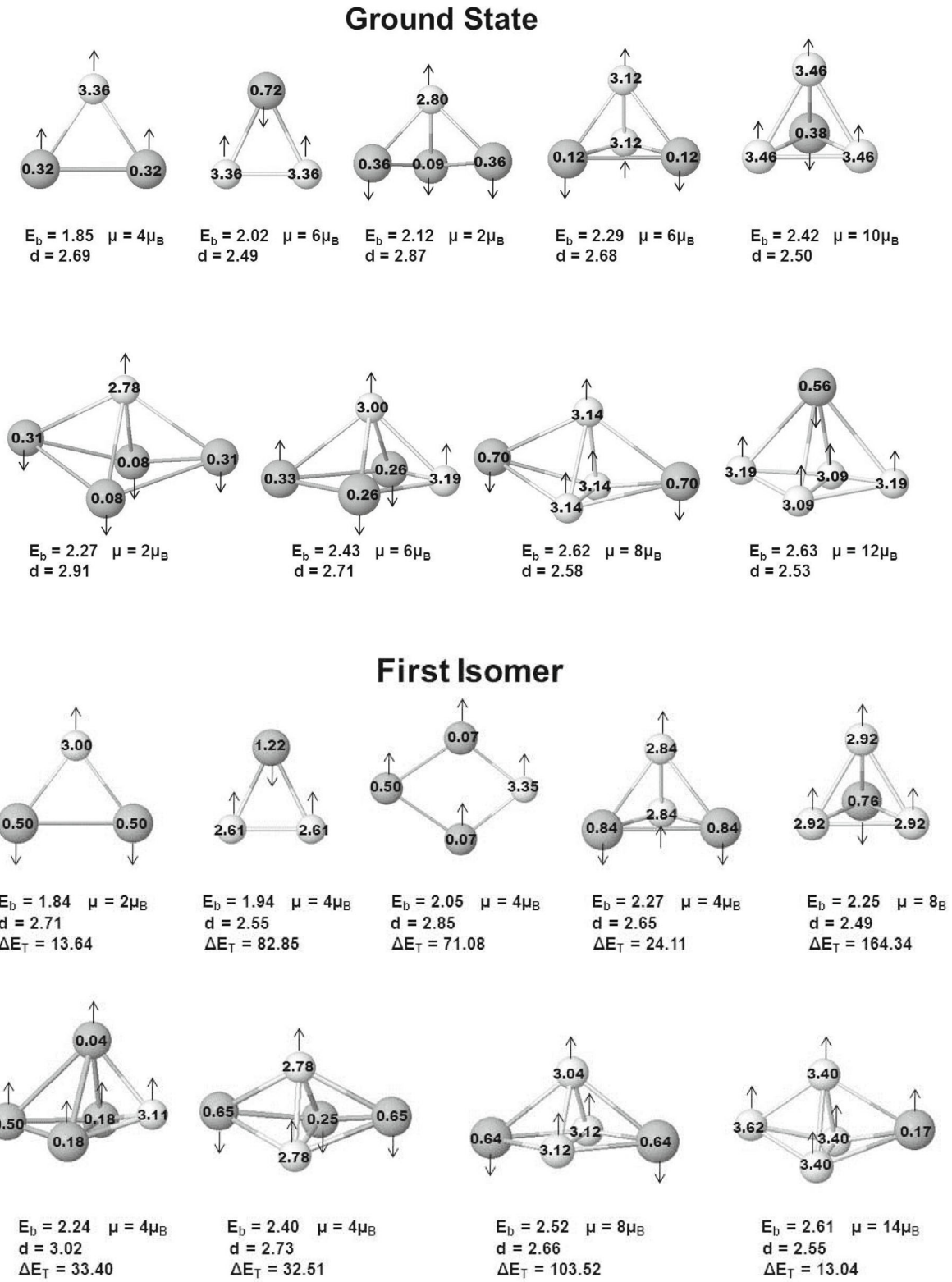

Fig. 2. Lowest energy structures of Fe_xSn_y as obtained in DFT calculations. ΔE_T is the total energy per atom relative to the ground state, G.S., ($\Delta E_T = 0$) in meV/atom, E_b is the binding energy per atom in units eV/atom. μ is the total magnetization and d represents the average bond lenght in units Å/bond the up and down arrows represent the direction of the atomic magnetic moment. White balls represent the Fe atoms, while the gray balls represent the Sn atoms.

derived from arguments on experimental results [12]. We can notice that the magnetization and the magnetic order into the cluster depend of chemical composition; in the first case the magnetic order is ferromagnetic-like, whereas in the second case is antiferromagnetic-like, in both cases the value of Fe magnetization does not change and represents the main contribution to the total magnetization of the clusters; from Figure 2, we can notice a large bond length in $FeSn_2$ cluster, this behavior is present in larger clusters doped with a Fe atom, see Figure 2. In the respective first isomers, the total magnetization is reduced in 2 μ_B with respect to the respective MES, in both structures the antiferromagnetic coupling is preserved.

For clusters with $x + y = 4$, all the MES present tetrahedrical structures, the same structure than for pure Fe_4 cluster, the planar structure is present only in the first isomer of $FeSn_3$ and is above of the ground state 71 meV/atom, see Figure 2. In this size, the antiferromagnetic-like order appears in all the ground states structures. The lowest value for μ(Fe) is in $FeSn_3$, and increases when the number of Fe atoms in the clusters increases too; besides for each Fe atom added the total magnetization increases in 4 μ_B, i.e., the magnetic moment of the Fe atom. In these clusters, the largest average bond length (d) is present in $FeSn_3$, where the main contribution comes from all the Sn-Sn bond lengths, the largest one is 3.39 Å, and two distances of 3.02 Å. It can be notice that d decreases when the number of Fe atoms in the cluster increases.

Some physical quantities are mantained for cluster with 5 atoms, for example the largest value of d for doped clusters with a Fe impurity, and the decreasing value of this distance when the number of Fe atoms increases in the cluster.

From Figure 2, the MES for doped clusters with 5 atoms present trigonal bipyramid mottifs, except for Fe_2Sn_3 whose global minimum structure is a non-regular square pyramid, where the Fe atoms have a different local environment giving as a result different values of μ(Fe), all the Sn atoms are in the base of the pyramid, but the magnetic order between them is not ferromagnetic-like. In the other clusters, all the μ(Sn) point in the same direction giving a ferromagnetic coupling between them.

From Figure 2, we can notice that some first isomers ($FeSn_3$, $FeSn_4$ and Fe_4Sn) present a total magnetization $2\mu_B$ higher than the respective MES, our results show a ferromagnetic-like order in these structures. The difference in total energy runs from 0.065 eV for Fe_4Sn to 0.35 eV for $FeSn_3$. The first result show two magnetic states quasi-degenerates, this fact has a consequence in the stability for this cluster.

3.3 Stability of the clusters

A central concept in any stability analysis of clusters is the binding energy per atom, which we define here for doped clusters as:

$$E_b(\mathrm{Fe}_x\mathrm{Sn}_y) = \frac{xE(\mathrm{Fe}) + yE(\mathrm{Sn}) - E(\mathrm{Fe}_x\mathrm{Sn}_y)}{x+y}, \quad (1)$$

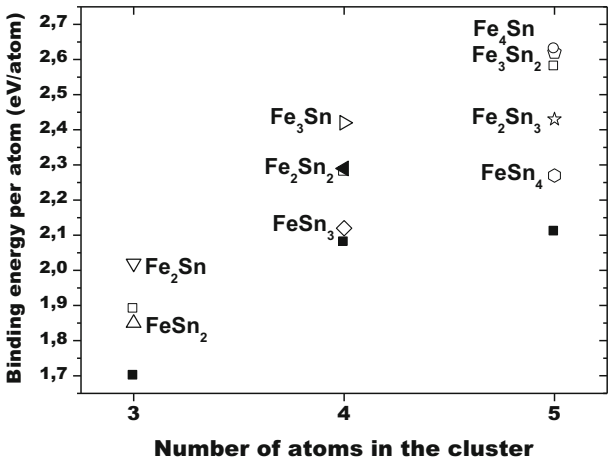

Fig. 3. Binding energy per atom for all the clusters studied here, the filled (unfilled) squares represent pure Sn (Fe) clusters.

and for pure clusters as:

$$E_b(M_n) = \frac{nE(M) - E(M_n)}{n}, \quad (2)$$

where E(M) (M = Fe, Sn) is the single atom energy for pure clusters, and $E(\mathrm{Fe}_x\mathrm{Sn}_y)$ is the total energy for doped clusters. The binding energies per atom for pure Sn and Fe clusters and nanoalloys of FeSn in the concentrations considered here as a function of the cluster size are plotted in Figure 3. We can notice general trends from this Figure; for pure clusters, the lowest value of E_b is present for all the pure Sn clusters, whereas for pure Fe structures their binding energy per atom is intermediate between Sn clusters and some $\mathrm{Fe}_x\mathrm{Sn}_y$ clusters.

For doped clusters with a Fe impurity, E_b takes the lowest value and from Figure 3 we can notice an increment of the binding energy per atom with the number of Fe atoms, and for doped clusters with a Sn atom in the clusters the largest value of E_b is present; we can notice, that for MES with the same number of Sn and Fe atoms ($x = y$), E_b takes almost the value than for the respective pure Fe_n clusters ($n = 2, 4$).

On the other hand, an index comparing the stability of binary clusters of nearby compositions may be useful. This index is the second difference in the energy $\Delta_2 E$ defined by:

$$\Delta_2 E(\mathrm{Fe}_x\mathrm{Sn}_y) = E(\mathrm{Fe}_{x+1}\mathrm{Sn}_{y-1}) + E(\mathrm{Fe}_{x-1}\mathrm{Sn}_{y+1}) - 2E(\mathrm{Fe}_x\mathrm{Sn}_y), \quad (3)$$

where all the terms on the right side are refered as the total energies of the clusters involved in the calculation. $\Delta_2 E$ compares sizes differing by one atom, clusters with high relative stability correspond to peaks in this index. For FeSn dimer, the value of $\Delta_2 E$ is 0.305 eV, indicating a relative stability in this structure. In Figure 4, we plot the second difference in the energy in terms of the number of Fe atoms in the clusters; for structures with 3 and 4 atoms present the same trend, the relative stability increases with the number of Fe atoms in the clusters and

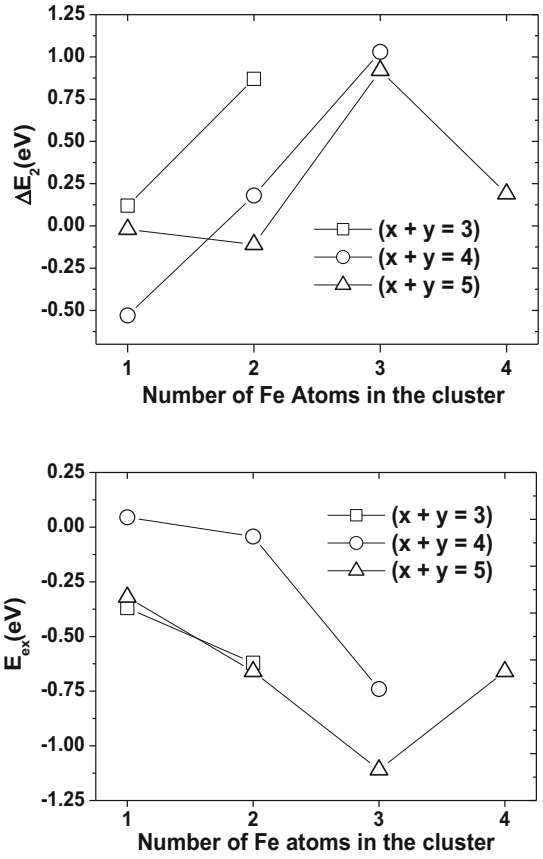

Fig. 4. Relative stability and excess energy for doped cluster, the upper pannel shows the relative stability, ΔE_2, and the lower pannel the excess energy, E_{ex}, both in eV and in terms of number of Fe atoms in the cluster.

the most stable stuctures correspond to clusters rich in Fe atoms, Fe_2Sn and Fe_3Sn, respectively.

Whereas for clusters with 5 atoms the most stable structure is Fe_3Sn_2; this change in the behavior of $\Delta_2 E$ is due to the large diference in the total energy between the MES and the first isomer as compared with the small difference in ΔE_T for Fe_4Sn cluster, see Figure 2.

In order to determinate the favorable mixing between Fe atoms with Sn atoms the excess energy defined by

$$E_{ex} = E(\mathrm{Fe}_x\mathrm{Sn}_y) - xE(\mathrm{Fe}_N)/N - yE(\mathrm{Sn}_N)/N, \quad (4)$$

is used i.e., substracting from the energy of the binary cluster the appropiate fraction of the total energy of pure reference clusters of the same size. In this way, E_{ex} is zero for pure clusters; in general a negative value of this excess energy indicates that mixing is favorable. For FeSn structure, the value of E_{ex} is -0.152 eV, indicating a favorable mixing. In the same Figure 4, we plotted E_{ex} in terms of the number of Fe atoms present in the clusters studied here; we can notice that mixing is favorable for the majority of clusters, except for $FeSn_3$ and Fe_2Sn_2 clusters; we can notice a same trend for E_{ex} that $\Delta_2 E$, the most favorable mixing is present in structures rich in Fe atoms or clusters with a Sn atom.

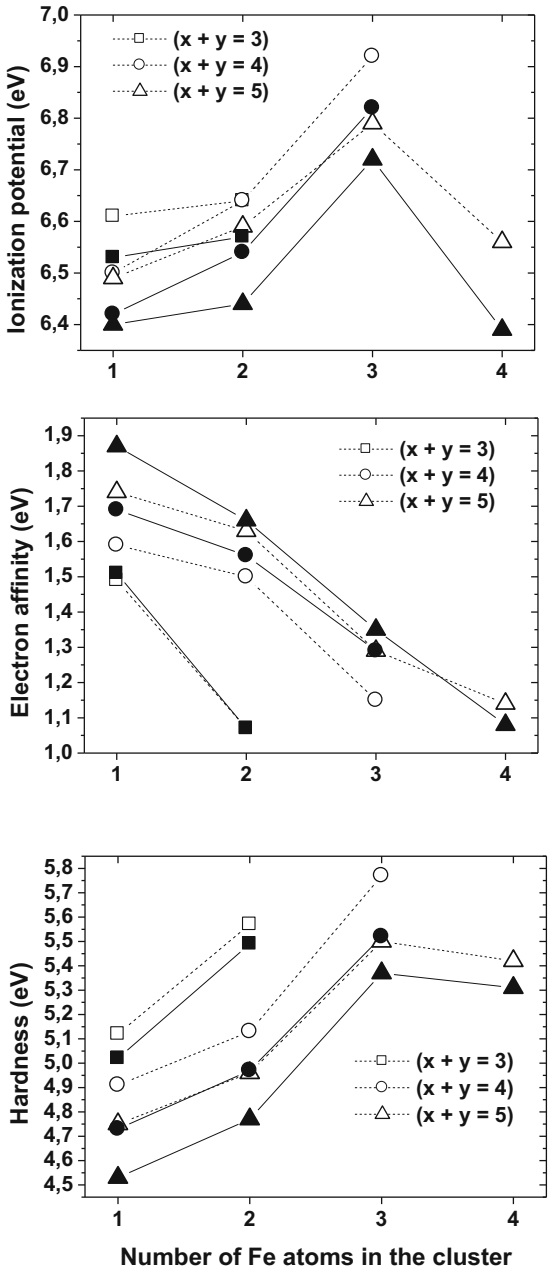

Fig. 5. Ionization potential, I, electron affinity, A, and hardness 2η, for all the structures studied here; the unfilled symbols correspond to vertical cases whereas filled symbols correspond to adiabatic cases.

3.4 Electronic properties of doped clusters

One concept related with the relative stability of the clusters is their chemical hardness defined by:

$$\eta = (I - A)/2, \quad (5)$$

where I and A are the ground state ionization potential and the electron affinity, respectively. We calculated both quantities vertically and adiabatically, see Figure 5. We can notice that I increases with the number of Fe atoms in the cluster, except for clusters with 5 atoms, where Fe_4Sn

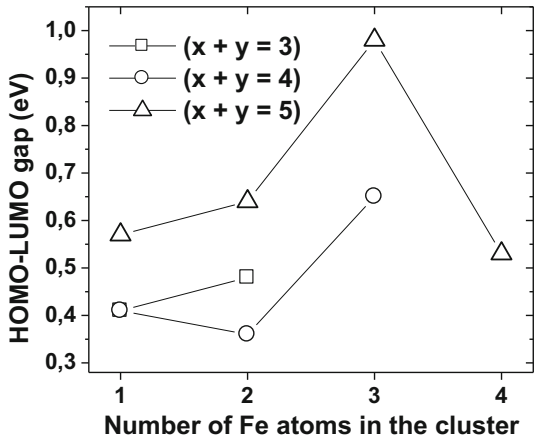

Fig. 6. Values for the HOMO-LUMO gap, for the lowest energy structures considered here.

cluster takes the lowest value; whereas the behavior of A is similar for all the clusters, decreases with the number of Fe atoms in the cluster. From these results, adding or removing one electron depends basically of the number of Fe atoms in the cluster.

In Figure 5, we present our results for η, we can notice that for clusters with 3 and 4 atoms, the maximum value of hardness is reached when the number of Fe atoms in the cluster takes the largest possible value in these sizes, but for structures with 5 atoms, the maximun value of η is reached in Fe_3Sn_2. These results are congruent with the results for ΔE_2, i.e., the maximum value of hardness reflects the maximum relative stability, see Figure 4.

In Figure 6, we show our results for the difference between the highest occupied molecular orbital and the lowest unoccupied molecular orbital, HOMO-LUMO gap (HLg); this quantity is an invaluable tool in the cluster stability study; we can see that the behavior of HLg is very similar to ΔE_2, i.e., for structures with 3 and 4 atoms the maximum value is reached when the number of Fe atoms is maximum in these clusters.

From these results, we do not find a correlation between HOMO-LUMO gaps with the binding energy per atom, see Figures 3 and 6.

4 Conclusions

In this work we performed DFT-GGA calculations of the structures, stability and electronic behavior of small binary Fe_xSn_y clusters with $x + y \leq 5$ atoms using the SIESTA code. Our results shown a favorable mixing and a high relative stability for the majority of the clusters studied here, mainly when the number of Fe atoms in the cluster increases; this behavior is reflected in the value of the hardness and in the HOMO-LUMO gap.

All the clusters show a magnetic behavior, where the total magnetization increases with the number of Fe atoms in the cluster, but is diminished as compared with the respective pure Fe cluster, due to the antiferromagnetic-like order among the Sn magnetization and the Fe magnetization, for structures with a Fe impurity, the main contribution for the total magnetization comes from the Fe atom.

We are grateful to Centro de Computo of Facultad de Ciencias, UASLP. All the authors contributed equally to the paper.

References

1. J.H. Sinfelt, *Bimetallic Catalysts: Discoveries, Concepts and Applications* (Wiley, New York, 1983)
2. K.C. Taylor, *Automobile Catalytic Converters* (Springer, New York, 1984)
3. L. Ferrando, J. Jellinek, R.L. Johnston, Chem. Rev. **108**, 845 (2008).
4. J.M. Montejano-Carrizales, F. Aguilera-Granja, J.L. Morán-Lopéz, Eur. Phys. J. D **64**, 53 (2011)
5. Z.J. Wu, Z.M. Su, J. Chem. Phys. **124**, 184306 (2006)
6. W.J. Zhao et al., Acta Physica Sinica **56**, 2596 (2007)
7. A. Hütten et al., J. Magn. Magn. Mater. **293**, 93 (2005)
8. R. Pal et al., J. Am. Chem. Soc. **131**, 3396 (2009)
9. V. Kumar, A.K. Singh, Y. Kawazoe, Nano Lett. **4**, 677 (2004)
10. Li Feng Chui et al., Angew Chem. **119**, 756 (2007)
11. F. Delogu, J. Phys. Chem. C **113**, 17059 (2009)
12. S. Shamai, M. Pasternak, H. Micklitz, Phys. Rev. B **26**, 3031 (1982)
13. E. Artacho, D. Sánchez-Portal, P. Ordejón, A. García, J.M. Soler, Phys. Stat. Sol. **215**, 809 (1999)
14. N. Troullier, J.L. Martins, Phys. Rev. B **43**, 1993 (1991)
15. L. Kleinman, D.M. Billander, Phys. Rev. Lett. **48**, 1425 (1982)
16. J.P. Perdew, K. Burke, M. Ernzerhof, Phys. Rev. Lett. **77**, 3865 (1996)
17. J. Izquierdo, A. Vega, L.C. Balbas, D. Sánchez-Portal, J. Junquera, E. Artacho, J.M. Soler, P. Ordejon, Phys. Rev. B **63**, 13639 (2000)
18. A. Lyalin, A.V. Solov'yov, W. Greiner, Phys. Rev. A **74**, 043201 (2006)
19. B. Assadollahzadeh, S. Schafer, P. Schwerdtfeger, J. Comput. Chem. **31**, 929 (2010)
20. K. Balasasubramanian, K.S. Pitzer, J. Chem. Phys. **78**, 321 (1983)
21. A.A. Shvartsburg, M.F. Jarrold, Phys. Rev. A **60**, 1235 (1999)
22. O. Díeguez, M.M.G. Alemany, C. Rey, P. Ordejón, L.J. Gallego, Phys. Rev. B **63**, 205407 (2001)
23. Q.-Ma, Z. Xie, J. Wang, Y.-Ch. Li, Solid. State. Commun. **142**, 114 (2007)
24. H. Purdum, P.A. Montano, G.K. Shenoy, T. Morrison, Phys. Rev. B **25**, 4412 (1982)
25. P.A. Montano, G.K. Shenoy, Solid State Commun. **35**, 53 (1980)
26. C.C. Yang, S. Li, J. Phys. Chem. C **113**, 14207 (2009)
27. C. Majumder, V. Kumar, H. Mizuseki, Y. Kawazoe, Phys. Rev. B **64**, 233405 (2001)
28. K.A. Gingerich, A. Desideri, D.L. Cocke, J. Chem. Phys. **62**, 731 (1975)
29. V.E. Bondybey, M. Heaven, T.A. Miller, J. Chem. Phys. **78**, 3593 (1983)
30. G. Meloni, W.R. Schmude Jr., J.E. Kingcade Jr., K.A. Gingerich, J. Chem. Phys. **113**, 1852 (2000)